ISSN 1392 - 1207. MECHANIKA. 2011. 17(5): 474-479

Effect of process parameters on mechanical behavior in hot-slab rolling

Licheng Yang*, Jinchen Ji, Jingxiang Hu***, A. Romagos******
**Department of Mechanical Engineering, Hunan Institute of Engineering, Xiangtan, China, E-mail: ylich2008@163.com*
***Faculty of Engineering, University of Technology, Sydney, NSW, Australia, E-mail: Jinchenji64@gmail.com*
****Department of Mechanical Engineering, Hunan Institute of Engineering, Xiangtan, China, E-mail: lelewcj@yahoo.com.cn*
*****Faculty of Engineering, University of Technology, Sydney, NSW, Australia, E-mail: Romago_A@yahoo.com.au*

1. Introduction

The hot continuous involves in material, geometry and contact nonlinearities, and it is difficult to obtain analytical solution. Trial-rolling method and physical experiment method have thus been often used to study rolling properties over the past decades at the expense of time and cost. Recently, 3D numerical simulation technology has been used to solve rolling problems based on FEM, as numerical simulation method can shorten development periods, and reduce the cost of research and development.

The study of rolling force and energy parameters in the hot rolling process has attracted a lot of attentions in the literature. For example, prediction of rolling pressure and rolling force of wire [1], calculation of rolling pressure of strip [2], simulation of stress and temperature [3], study of plastic deformation of strip [4, 5], and discussion of strain and stress. FEM method and numerical simulations have been proved to be a very powerful tool for prediction of rolling force and energy parameters in rolling process. Some commercial software packages have also been used to simulate the rolling process, for example, the program FORGE3 [6]. The effect of rolling parameters on the rolling properties has not yet been fully understood. The effect of rolling parameters on temperature [7], friction stress, rolling force [8, 9], and effective stress and strain [10] were discussed. Friction is the reason for the rolling process to actually take place. It acts as the driving force and has major effect on the product quality and the stability of rolling process. Some researchers studied the effect of reduction [11], width spread [12], and frictional coefficient [13] on the distribution of temperature, stress, and separating force using the frictional shear stress model. To improve calculation accuracy, stiffness of frictional element was corrected by the thickness of frictional element and friction factor [14].

In the present paper, the hot rolling process of a slab is studied by using the rigid-plastic finite element method. The 2D models of the roll and the slab are developed to investigate the effect of different process parameters such as initial rolling temperature, slab thickness, rolling speed, friction coefficient, and reduction rate on the rolling force, normal force, and effective stress distribution. Moreover, friction distribution in the deformation zone is also studied based on 3D models.

2. Modeling

2.1. Analytical formula of rolling force

The microelement body in the deformation zone was usually employed to develop the modeling of rolling force, as shown in Fig. 1.

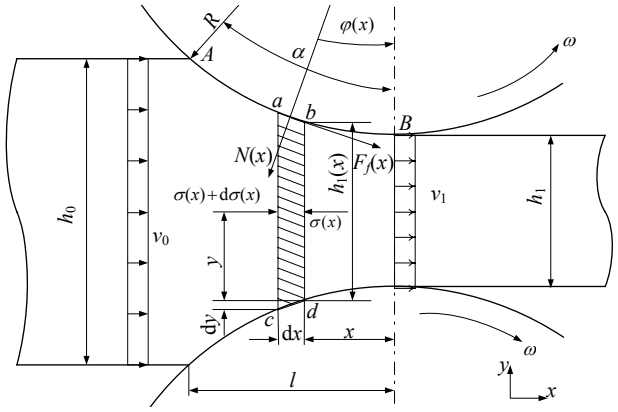

Fig. 1 Geometry of slab rolling process

Under the basic assumptions and equilibrium conditions, the analytical equation of unit force (Karman equation) is obtained based on any microelement body (*abcd*) in the deformation zone.

$$\frac{dN(x)}{dx} - \frac{K}{y}\frac{dy}{dx} \pm \frac{F_f(x)}{y} = 0 \tag{1}$$

where $N(x)$ is unit force, K is metal natural intensity and $F_f(x)$ is unit friction. It is assumed that contact condition in the deformation zone obeys Coulomb friction model. If the chord is used to represent the contact arc, the distribution of unit pressure can be expressed as

$$N(x) = \frac{K}{\delta}\left[(\delta \mp 1)\left(\frac{h_0}{h_1(x)}\right)^{\delta} \pm 1\right] \tag{2}$$

where $\delta = 2lf/\Delta h$, Δh is reduction rate, h_0 is initial workpiece height, and $h_1(x)$ is the height after rolling. It is found that the main factors affecting unit pressure are friction coefficient, roller diameters, reduction rate, workpiece height and tensile force. In fact, the hot rolling of slab belongs to typical thermo-mechanical coupled problem. To describe the relation, the equation shows

$$\begin{bmatrix} 0 & 0 \\ 0 & [C] \end{bmatrix} \begin{Bmatrix} \{\dot{u}\} \\ \{\dot{T}\} \end{Bmatrix} + \begin{bmatrix} [K] & 0 \\ 0 & [\Lambda] \end{bmatrix} \begin{Bmatrix} \{u\} \\ \{T\} \end{Bmatrix} = \begin{Bmatrix} \{F\} \\ \{Q\} \end{Bmatrix} \tag{3}$$

where $[C]$, $[K]$ and $[\Lambda]$ are specific heat matrix, stiffness matrix and conductivity matrix, respectively, $\{u\}$, $\{T\}$, $\{F\}$ and $\{Q\}$ are the vectors of displacement, temperature, structural load and heat flow, respectively. The governing partial differential denotes

$$\frac{\partial}{\partial x_i}\left(\lambda_{ij}\frac{\partial T}{\partial x_j}\right) + \dot{q} - \rho c\frac{\partial T}{\partial t} = 0 \tag{4}$$

where $\dot{q}$, ρ, c, t and λ_{ij} are heat generation rate per unit volume, density, specific heat, time and thermal conductivity coefficient, respectively. The following conditions are used to solve Eq. (4).

1. Initial and boundary conditions

$$T(y,t) = T_0 \quad (t=0), \quad \frac{\partial T(y,t)}{\partial y} = 0 \quad (y=0) \tag{5}$$

where T_0 shows initial workpiece temperature.

2. Heat generation due to plastic deformation and friction work.

$$\dot{q}_{def} = \eta\bar{\sigma}\dot{\bar{\varepsilon}}, \quad q_f = \sigma_\tau A_c v_r \delta t \tag{6}$$

where $\dot{q}_{def}$, $\bar{\sigma}$, $\dot{\bar{\varepsilon}}$ and η are heat generation due to plastic deformation, effective flow stress, effective strain rate and conversion efficiency of deformation energy to heat, respectively. Friction work also can generate heat along the contact arc, which results in changing significantly temperature in forward/backward slip zones. In Eq. (6), q_f, A_c, δt, σ_τ and v_r are heat generation due to friction work, contact area, time increment step, friction shear stress and relative sliding velocity, respectively.

3. Heat loss due to thermal exchanges. The main thermal exchanges include conductivity, convection, radiation, and water cooling, which causes the metal surface be cooled and conversely the rolls gain heat

$$\left.\begin{aligned} q_1 &= \lambda(T_s - T_r), \quad q_w = h_w(T_s - T_w) \\ q_2 &= h_c(T_s - T_a) + \sigma_{st}\varepsilon_r(T_s^4 - T_a^4) \end{aligned}\right\} \tag{7}$$

where q_1, q_2 and q_w are heat loss of the metal by conductivity, convection and radiation, and the forced convection of water, respectively λ, h_c and h_w are conductivity coefficient, convective coefficient and heat transfer coefficient for water cooling, respectively. T_s, T_r, T_a and T_w show the temperature of workpiece, roll, air and water, respectively. σ_{st} is Stenfan-Boltzmann constant, and ε_r is the surface emissivity.

2.2. Material properties

To reduce the computational time, only one half of the geometric model is considered in numerical simulation due to rolling symmetry. The meshes are very dense in the contact zone, as shown in Fig. 2. Thermo-mechanical coupling FEM and isoparametric technology are used to develop the models. The rolls are assumed to be rigid and heat transfer body, and their material is an iron steel of high chromium and the chemical composition is given as: 1.5% C, 0.75% Si, 0.67% Mn, 5.5% Cr, 2.6% Mo, 1.43% V and 1.82% W. The workpiece material is a typical carbon steel and its chemical composition is defined as follows: 0.14% C, 0.62% Mn, 0.27% Si, 0.032% P and 0.041% S. It obeys Von Mises yield criterion and the flow rule. Uniform temperature distribution is assumed throughout the original workpiece. The density of the material is 7850 kg/m^3 and the Poisson's ratio is 0.3. The material's elastic module, heat expansion factor, heat conduction rate and specific heat are the function of temperature.

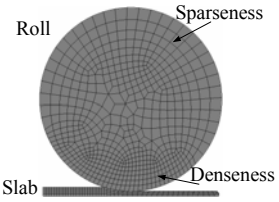

Fig. 2 The finite element meshes of the slab and the roll

3. Results and discussion

3.1. Effect of initial workpiece temperature and reduction on rolling force

For the slab rolling, the variation of rolling force F with initial workpiece temperature T_0 and reduction rate r is shown in Fig. 3. It is seen that F reduces with the increasing T_0. Moreover, when T_0 attains certain value, i.e. approximate 1200°C, F remains invariable even with the continuous increase of temperature. If other conditions are kept unchanged, the increasing r will increase the length of contact arc and unit pressure. This in turn causes an increase of F applying on the roll, which results from the increase of contact area and the increase of unit pressure. By comparing reduction rate r 20%, 30% and 40% with the reduction rate of 10%, the rolling force increases by 83%, 156% and 226% for the same T_0 1000°C, respectively.

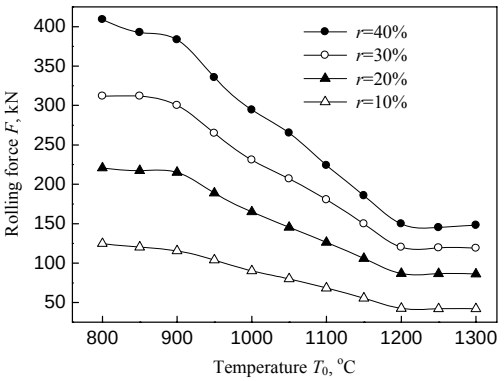

Fig. 3 Effect of workpiece temperature and reduction on rolling force

3.2. Effect of friction coefficient and roll's radius on rolling force

Fig. 4 shows the variation of rolling force F with friction coefficient f and roll's radius R. When f increases, the unit pressure p increases fast from the entry and exit position to neutral point (a point where shear stress

changes its sign). Accordingly, the total pressure of the workpiece applying on the roll also increases. F rises with the increasing R. It can be explained that the length of contact arc L and p will increase with the increasing R. By comparing R 400 mm, 500 mm and 600 mm with R 300 mm, F increases by 12%, 25% and 39% for the same f 0.3, respectively.

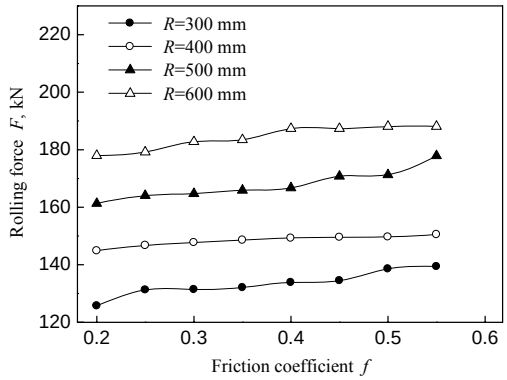

Fig. 4 Effect of friction coefficient and roll radius on rolling force

3.3. Effect of rolling speed on rolling force

Fig. 5 shows the effect of rolling speed v on rolling force F. It is found that the larger v or rotational angular speed ω is, the bigger then F is, and the rolling force curve is more remarkable. Rolling time is shorter when the value of v or ω is larger. By comparing speed 500 mm/s with 5000 mm/s, there are more peak forces for the lower speed case under the same time step. For example, for No. 188 time increment steps and 0.0002 s per time step, there are 13, 8, 5 and 2 peak forces, respectively. Rolling speed leads to increase the deforming process of the workpiece, and the metal plasticity reduces in the deformation zone. If rolling speed is too high, metal flow speed will increase along rolling and spread directions. The effect of forming then becomes poor and reduces the product quality.

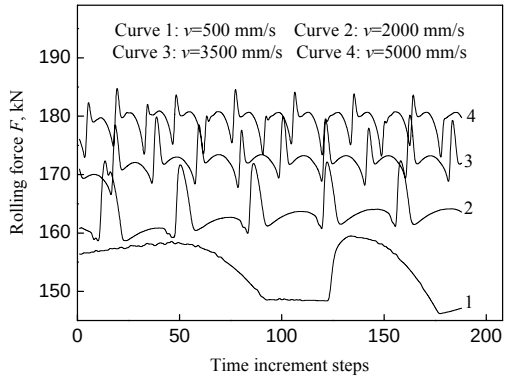

Fig. 5 Effect of rolling speed on rolling force

3.4. Effect of workpiece thickness on rolling force

Under the condition of the same other parameters, the effect of different entry thickness h_0 of the slab on the rolling force is shown in Fig. 6. It is observed that the contact pressure between the slab and the roll increases in the hot rolling process when initial thickness of the slab decreases. When the reduction rate keeps the same, h_0 is smaller and its deformation is more severe. The curve of rolling pressure reveals multiple pressure peaks in existence, and the amplitude of the rolling force increase with the decreasing h_0. When the reduction value Δh equals to 20 mm, the rolling force reduces by 33%, 42%, 48% and 52%, respectively, comparing the initial thickness h_0 40 mm, 50 mm, 60 mm and 70 mm with the thickness 30 mm.

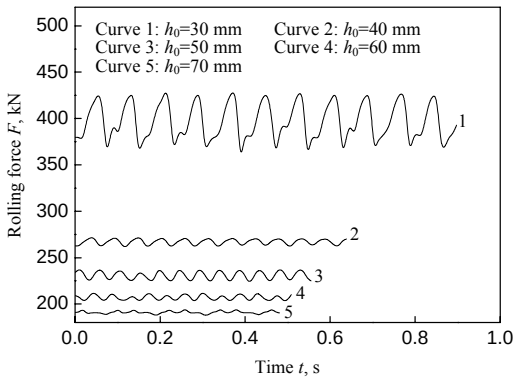

Fig. 6 Effect of initial workpiece thickness on rolling force

3.5. Stress distribution

In hot rolling process, strain, strain rate and temperature can affect stress distribution in the deformation zone.

1. The lowest temperature of the slab occurs at the exit of the deformation zone because the position is in the contact with the roll for more time, which results in more heat loss.

2. The maximum strain rate generally is produced in the entry position of the deformation zone because the deformation occurs in this zone suddenly.

3 Large plastic deformation occurs in the contact zone because the continuous deformation and flow of mental occurs along rolling direction and spread direction. It is observed from Fig. 7 that the maximum effective stress occurs under the roll and at the contact zone. This indicates that the effect of strain is dominant.

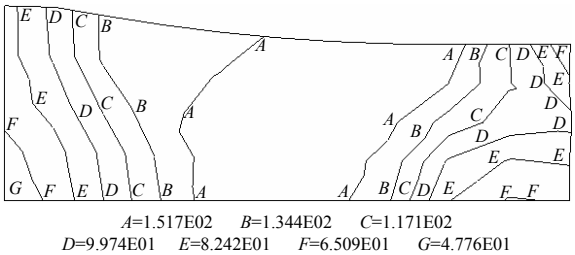

Fig. 7 Distribution of effective stress in the deformation zone

3.6. Effect of tension on rolling force

Tension is a major phenomenon in continuous rolling process. It is produced by noncompatibility velocities or reduction among tandem mills. For the multitandem mills (Fig. 8), the tension increases if the exit velocity of stand I (v_{I}) is reduced and the entry velocity of stand II (v'_{II}) increases. When v_{I} drops, the corresponding forward slip

quantity $((v_I - R_I\omega_I)/ R_I\omega_I)$ decreases due to the variations of roll speed ($R_I\omega_I$) or other process parameters, for example, reduction rate (r_I). In addition, when v'_{II} increases because of the increasing roll speed ($R_{II}\omega_{II}$) or the drop of the backward slip magnitude ($(vcos\alpha-v_H)/vcos\alpha$), where α is the biting angle (Fig. 1), thus these cause the slab between mill I and mill II tauten and the increase of the tension.

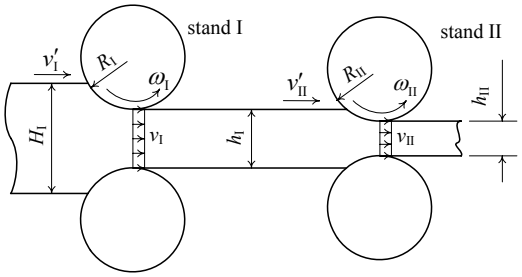

Fig. 8 The parameters for multi-tandem mills

Fig. 9 shows that the rolling force varies with tension. The curves I_1 and II_1 represent rolling forces of two mills for the case of tandem mill I and tandem mill II satisfying Rule of Volume Flow Rate (The volume flow of the front mill equals to that of the back mill per unit time), while the curves I_2 and II_2 for the case that there is the phenomenon of pulling steel between mill I and mill II. The curves show the rolling forces reduce significantly with an increase of tension. The rolling force is smaller if tension is bigger. Tension rolling is thus recommended in actual rolling process. Moreover, if the exit velocity of mill I (v_I) increases or the entry velocity of mill II (v'_{II}) decreases, there is the phenomenon of pushing steel between mill I and mill II, and thus the tension drops. This causes the rolling forces of two tandem mill to increase dramatically, as shown in the curves I_3 and II_3.

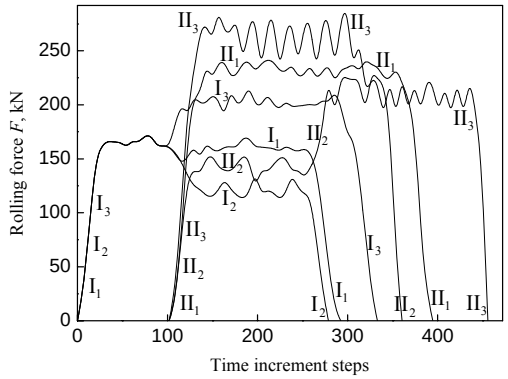

Fig. 9 Effect of tension on rolling force, curve I_1, I_2, I_3 - rolling force of mill I: curve II_1, II_2, II_3 - rolling force of mill II

3.7. Friction distribution

For a given normal force, friction force has a step function behavior based upon the relative sliding velocity. Since this discontinuity in the friction value causes numerical difficulties, an updated Coulomb model is used

$$f_\tau = -mf_n \frac{2}{\pi} tan^{-1}\left(\frac{\|v_r\|}{v_0}\right)\frac{v_r}{\|v_r\|} \quad (8)$$

where f_τ is tangential friction force, f_n and m denote contact normal force and friction factor, respectively. v_r is the relative sliding velocity and v_0 is a small positive number. Fig. 10 shows 3D finite element models of rolling process and friction distribution. The other parameters of material are identical to those of 2D model. Along rolling direction, F_f is negative in forward slip zone where the exit velocity of the workpiece v_1 (Fig. 1) is more than the linear velocity of the roller v. It indicates that friction force direction is the opposite of rolling direction, moreover, F_f is positive in backward slip zone where the entry velocity of the slab v_0 is less than the horizontal component of the linear velocity of the roller $v\ cos\ \alpha$. From Fig. 10, the maximum positive friction force 79.52 kN is more than the maximum negative friction 74.39 kN along the rolling direction. The area of the positive friction zone is bigger than the negative friction zone. It indicates that friction force is the driving force and is also the reason for the process of rolling to actually take place. There is the sticking zone between positive and negative friction, i.e., friction and relative sliding velocity all equal to zero.

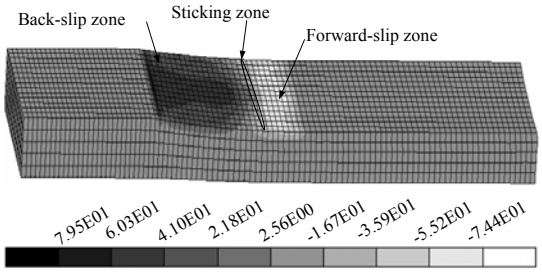

Fig. 10 Friction distribution of the deformation zone

It can be seen from Fig. 11 that friction force curve divides into the positive friction force zone and the negative force zone. For example, for reduction rate 20%.

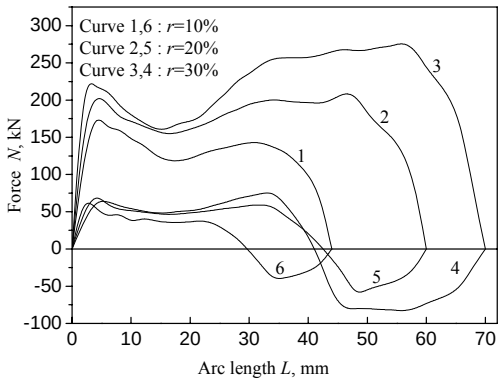

Fig. 11 Effect of reduction rate on friction force and contact normal force. Curve *1*, *2*, *3* - contact normal force; curve *4*, *5*, *6* - friction force

The positive friction force (L 42 mm) is more than the negative friction force (L 18 mm) along rolling direction, moreover, the maximum positive force and the maximum negative friction force equal to 74.727 and 62.174 kN, respectively. It is observed that an increasing relative reduction rate can improve L and unit pressure p under the condition of invariable other parameters. L increases from 44 to 70 mm and the backward slip zone increases from 14 mm to 28 mm when r increases from 10 to 30%, and it causes an increase of F_f and F. By comparing r

10 and 30 with *r* 10%, the maximum normal force increases by 13.51 and 32.38%, respectively, and this keeps the same with the results of Shahani [15].

4. Conclusions

Based on thermo-mechanical coupled FEM, a mathematical model has been developed to predict flow stress, rolling force, contact normal force and friction force during hot continuous rolling process. The simulation results were found to be in good agreement with the reported results in the theoretical analysis and experiment measurements in the literature. The conclusions have been obtained and verified by numerical simulation for the hot rolling process.

1. An increase of the initial slab temperature and thickness will reduce the rolling force. Temperature, train and train rate have major effect on stress distribution and the effect of strain is dominant.

2. When the percentage reduction, work-roll radius, friction coefficient and rolling speed increase, the corresponding energy-force parameters increase.

3. The positive friction is more than the negative friction, suggesting that friction acts as the driving force in the rolling process.

Acknowledgements

The work was supported by project 51004047 of NSFC; Project 10B020 of Hunan Provincial Education Department; and project 09jj4024 of NSF of Hunan.

References

1. **Kazeminezhad, M.; Taheri, K.A.** 2006. Calculation of the rolling pressure distribution and force in wire flat rolling process, J. Mater. Process. Manuf. Sci. 171(2): 253-258.
2. **Liu, X.H.; Shi, X.; Li, S.Q.; Xu, J.Y. et al.** 2007. FEM analysis of rolling pressure along strip width in cold rolling process, J. Iron Steel Res. Int. 14(5): 22-26.
3. **Kim, S.Y.; Im, Y.T.** 2002. Three-dimensional finite element analysis of non-isothermal shape rolling, J. Mater. Process. Technol. 127(1): 57-63.
4. **Zhang, G.M.; Xiao, H.; Wang, C.H.** 2006. Three-dimensional model for strip hot rolling, J. Iron Steel Res. Int. 13(1): 23-26.
5. **Parsa M.H.; Mazaheri, H.** 2009. Finite element and experimental deformation analysis of NiTi alloy during rolling, Int. J. Mater. Form. 2: 13-16.
6. **Duan, X.; Sheppard, T.** 2009. Three dimensional thermal mechanical coupled simulation during hot rolling of Aluminium alloy 3003, Int. J. Mech. Sci. 44(10): 2155-2172.
7. **Serajzadeh, S.** 2008. Effects of rolling parameters on work-roll temperature distribution in the hot rolling of steels, Int. J. Adv. Manuf. Technol. 35(9-10): 859-866.
8. **Garber, E.A.; Kozhevnikova, I.A.; Tarasov, P.A.; et al.** 2007. Effect of sliding and rolling friction on the energy–force parameters during hot rolling in four-high stands, Russ. Metall. 2007(6): 484-491.
9. **Lenard, J.G.** 2004. The effect of roll roughness on the rolling parameters during cold rolling of an Aluminum alloy, J. Mater. Process. Technol. 152(2): 144-153.
10. **Yang, L.C.; Hu, J.X.; Ning, L.W. et al.** 2009. Research on influence of rolling parameters on the rolling process based on numerical simulation, Int. J. Modell. Identi. Control. 7(1): 25-32.
11. **Jiang, Z.Y.; Tieu, A.K.; Lu, C. et al.** 2004. Three-dimensional thermo-mechanical finite element simulation of ribbed strip rolling with friction variation, Fin. Elem. Anal. Des. 40(9-10): 1139-1155.
12. **Jakstas, M.** 2010. The investigation of fuel consumption of the ICE with traditional and modified work cycle, Mechanika 83(3): 64-67.
13. **Gudur, P.P.; Salunkhe, M.A.; Dixit**, **U.S.** 2008. A theoretical study on the application of asymmetric rolling for the estimation of friction, Int. J. Mech. Sci. 50(2): 315-327.
14. **Du, F.S.; Wang, G.G.; Zang, X.L. et al.** 2010. Friction model for strip rolling, J. Iron Steel Res. Int. 17(7): 19-23, 43.
15. **Shahani, A.R.; Setayeshi, S.; Nodamaie, S. A. et al.** 2009. Prediction of influence parameters on the hot rolling process using finite element method and neural network, J. Mater. Process. Manuf. Sci. 209(4): 1920-1935.

Licheng Yang, Jinchen Ji, Jingxiang, A.Romagos

KARŠTOJO VALCAVIMO PROCESO PARAMETRŲ ĮTAKA MECHANINĖMS CHARAKTERISTIKOMS

R e z i u m ė

Straipsnyje nagrinėjamas tipiško mažaanglio plieno karštojo valcavimo procesas naudojant tamprių plastinių baigtinių elementų metodą. Skaitinis modelis nagrinėjama plonėjimo laipsnio, valcavimo spindulio, trinties koeficiento, valcavimo greičio, tempimo, pradinės valcavimo temperatūros ir pradinio plokštės storio įtaką valcavimo jėgai ir plokštės deformacijėms charakteristikoms. Nustatyta, kad valcavimo jėga didėja didėjant plonėjimo laipsniui, valcavimo greičiui, trinties koeficientui ir spinduliui. Pradinė valcavimo temperatūra, pradinis plokštės storis ir tempimas turi didelę įtaką valcavimo jėgai, kuri gali gerokai sumažėti didėjant išvardintiems parametrams. Be to, nustatyta, kad valcavimo jėga nekinta, kai pradinė plokštės temperatūra pasiekia tam tikrą ribą. Nustatyta trintis ir efektyviųjų įtampų pasiskirstymas plokštėje stabilios būsenos valcavimo procese. Nustatytas teigiamas trinties poveikis užpakalinėje slydimo zonoje; jis yra didesnis už neigiamą trinties poveikį priešakinėje slydimo zonoje išilgai valcavimo krypties. Tai rodo, kad trintis valcavimo procese veikia kaip stimuliuojanti jėga.

Licheng Yang, Jinchen Ji, Jingxiang Hu, A Romagos

EFFECT OF PROCESS PARAMETERS ON MECHANICAL BEHAVIOR IN HOT-SLAB ROLLING

S u m m a r y

This paper studies hot rolling process of typical low carbon steel by using rigid-plastic finite element

method. Numerical simulations are carried out to examine the effects of the percentage of reduction rate, work-roll radius, frictional coefficient, rolling speed, tension, initial rolling temperature and initial slab thickness on rolling force and deformation behavior of the slab. It is found that rolling force increases with the increases of reduction rate, rolling speed, frictional coefficient and radius. The initial rolling temperature, initial slab thickness and tension have also important effects on rolling force, and it will decreases remarkably by increasing the parameters. Moreover, it is also found that rolling force remains unchanged when initial slab temperature reaches certain value. The friction and effective stress distribution in the slab are obtained for the steady-state rolling process. The positive friction in backward slip zone is found to be greater than the negative friction in forward slip zone along rolling direction, indicating that friction acts as the driving force in the rolling process.

Received March 30, 2011
Accepted September 30, 2011